Precision of Spacecraft Doppler Tracking at Low Signal-to-Noise Ratios

D. R. Buccino[1] , K. Oudrhiri[1], M. Parisi[1], R.S. Park[1], E. Mazarico[2], P. Tortora[3,4], P. Withers[5], A. Genova[6], M. Zannoni[3,4]

[1] Jet Propulsion Laboratory, California Institute of Technology

[2] Goddard Space Flight Center, National Aeronautics and Space Administration

[3] Department of Industrial Engineering, Alma Mater Studiorum - Università di Bologna, Italy

[4] Centro Interdipartimentale di Ricerca Industriale Aerospaziale, Alma Mater Studiorum - Università di Bologna, Italy

[5] Boston University, Boston, MA

[6] Dipartimento di Ingegneria Aerospaziale e Astronautica, Universita` di Roma "La Sapienza," Rome, Italy

Corresponding author: Dustin R. Buccino (Dustin.R.Buccino@jpl.nasa.gov)

Key Points:

- Spacecraft Doppler measurements can be acquired at low signal-to-noise ratios with open-loop receivers
- Experiments with Deep Space Network ground systems show Dopper data with a signal-to-noise ratio as low as ~4 dB-Hz can be used
- Typical Doppler measurements at low SNR maintain a line-of-sight velocity precision of <0.1 mm/s at 60-second integration time

Abstract

The signal-to-noise ratio received at Earth is typically larger than 10 dB-Hz for radio tracking of a spacecraft in deep space, allowing a phase-locked loop to execute reliable carrier tracking. Recently, missions have been proposed to utilize low-gain antennas for Doppler tracking where the signal-to-noise ratio may be at the single-digit (dB-Hz) level. In this work, we discuss spacecraft Doppler tracking at these low signal-to-noise ratios through an analysis of thermal noise on the radio link, results from ground testing with the Deep Space Network, and demonstrations with an active spacecraft. We show that by utilizing an open-loop receiver to capture the carrier signal and by applying post-processing techniques, radio data with the signal-to-noise ratio as low as 4 dB-Hz can be used to derive Doppler data with precision sufficient for tracking a spacecraft in deep space.

Plain Language Summary

Typical deep-space probes utilize High Gain Antennas for radio tracking that enable large signal-to-noise ratios despite the long distances from Earth. When a Low Gain Antenna is used instead, the signal-to-noise ratio is decreased, resulting in increased thermal noise and questions about the ability to track. This work shows that signals can be tracked with the Deep Space Network's Open Loop Receiver down to 4 dB-Hz with sufficient precision for radio science experiments.

1 Introduction

Radio links between spacecraft in deep space and Earth-based radio telescopes has been used for decades to aid in the navigation of spacecraft, and to investigate planetary atmospheres, ionospheres, surface properties, and interior structure (Asmar et al., 2019). By tracking the carrier frequency of the radio signal sent by a planetary spacecraft, one can measure the Doppler shift caused by the relative motion between the spacecraft and the ground antenna. This measurement, referred to as the Doppler observable or carrier frequency observable, is widely used in spacecraft navigation and radio science experiments.

The National Aeronautics and Space Administration's (NASA) Deep Space Network (DSN) is a set of large-aperture (34-meter or 70-meter) ground stations used for communication and navigation of spacecraft beyond the orbit of the Moon. A typical application of the radio link involves a sizable (>2m) High-Gain Antenna (HGA) on the spacecraft transmitting to the large-aperture dishes of the DSN equipped with cryogenically-cooled low-noise amplifiers. This often results in a radio carrier signal-to-noise ratio (SNR) of >10 dB-Hz with typical values ~40 dB-Hz. The DSN's closed-loop receiver utilizes a phase-locked loop (PLL) to track the carrier signal, requiring an SNR >10 dB-Hz with a 1 Hz loop-bandwidth to track (O'Dea and Kinman, 2019).

Recently, missions have proposed using wide-beamwidth Low Gain Antennas (LGAs) to allow tracking a spacecraft's radio carrier and conduct radio science observations that could otherwise not be accomplished with a body-fixed HGA due to pointing constraints onboard the spacecraft (e.g., Mazarico et al., 2021 and Dehant et al., 2020). The resulting SNRs would be in the low single-digits (dB-Hz). This low-SNR precludes the use of the typical closed-loop receiver. Thus, any data collected at these levels would need to rely on the DSN's Open Loop Receiver (OLR) which is used in numerous radio science, radio astronomy, very long baseline interferometry, delta-differential one-way ranging, and engineering applications (Bedrossian &

Rogstad, 2021). The OLR records the downconverted antenna voltages as In-phase and Quadrature (IQ) samples. The receiving team would process these IQ samples into typical tracking observables such as the Doppler observable. This article demonstrates the capabilities of the DSN's Open Loop Receiver (OLR) to capture, detect, and process a precise Doppler observable at these low-SNR levels (<10 dB-Hz).

2 Previous Use of Low-SNR Signals

Previously, deep-space missions have conducted radio Doppler tracking using LGAs at low SNR. However, typically these data are only used as the prime data set if either the SNR is large enough to track with the closed-loop receiver reliably, or as a part of a measurement that requires the OLR such as radio occultation or bistatic scattering experiments. LGAs have previously been utilized for gravity science measurements; recent examples include Juno at Jupiter, Cassini at Titan, Dawn at Vesta and Ceres, and MESSENGER at Mercury.

Juno's gravity science investigation primarily utilizes dual-frequency links through an HGA, but the mission plan called for closest-approach periods with off-Earth pointing. During these, it was decided to track the spacecraft at a single-frequency with either a Medium Gain Antenna (MGA) or LGA to get additional Doppler tracking to supplement the prime gravity science data. An example of this is Juno's PJ-04 flyby on 07 February 2017. An average SNR of 10.7 dB-Hz on the 34-meter DSS-25 antenna was observed. The closed-loop receiver could not track the signal due to the MGA's low SNR and Doppler spin signatures (Buccino et al., 2018b).

Cassini conducted one flyby of Titan while utilizing the spacecraft's LGA on 16 March 2015 ("T110"). That experiment had been prepared by a previous test, carried out on 15 August 2010, which showed the feasibility of gravity measurements using the LGA (Barbaglio et al., 2012). Due to the significant Earth-Saturn distance and low link margin calculated by the telecommunications engineers, in order to acquire a lock on the spacecraft a special maneuver was added to bring the LGA antenna closer to boresight only during uplink acquisition to the spacecraft transponder. After the coherent link was established, the spacecraft transponder retained the lock. During the flyby, the SNR was variable between ~10-20 dB-Hz due to spacecraft pointing and scanning maneuvers required by other instruments (Barbinis, 2016). The data acquired during T110 were successfully used to retrieve the gravity field and ephemerides of Titan (Durante et al., 2019; Lainey et al., 2020).

Dawn utilized radio tracking to determine the gravity fields of Vesta and Ceres. The HGA tracking was supplemented with LGA tracking to increase the amount of Doppler data for the gravity field investigation. The SNR on the LGAs was predicted to be ~22-24 dB-Hz at a 70-meter DSN antenna, so that the corresponding Doppler quality was adequate for gravity recovery (Konopoliv et al., 2011).

The use of LGAs in radio occultations is rarer. MAVEN has a limited number of opportunities to conduct carrier-only radio occultation observations using the HGA, which requires an Earth-pointed orientation and no telemetry on the downlink signal. The number of observations was increased by a factor of 2-3 by also conducting telemetry-on observations using the LGA in which Earth-pointing requirements are significantly relaxed and telemetry can be included on the downlink signal. Furthermore, as LGA observations are not confined to MAVEN's biweekly dedicated communication periods, multiple observations can be acquired daily in support of investigations of time-variable phenomena in the environment of Mars (Felici

et al., 2020). Withers et al. (2020) generated vertical profiles of ionospheric electron density from these observations and reported average uncertainties of 1900 cm-3 and 2700 cm-3 for HGA and LGA observations, respectively. These are proportional to the average uncertainties in the frequency residual. Galileo also performed gravity and occultation experiments on its LGA after the deployment failure of the HGA, with limitations (Hinson et al., 1997).

3 Thermal Noise

Doppler noise budgets for deep-space probes are well-understood and quantified (Asmar et al., 2005; Iess et al., 2014). Typical noise sources for precision Doppler measurements include instrumentation noise (frequency and timing, ground electronics, antenna mechanical noise, spacecraft electronics/oscillators, thermal noise) and propagation noise (solar and planetary plasma, Earth ionosphere, Earth troposphere). Using a coherent two-way link, one where the downlink signal is phase-coherent with the uplink signal, the frequency reference is provided by the highly-stable hydrogen maser clocks from the DSN frequency and timing system and onboard spacecraft oscillator noise is not contributing. This is the type of measurement (coherent two-way) typically performed for gravity science studies where signal stability is a crucial factor. In this configuration, dominating noise sources are typically solar plasma and Earth troposphere scintillation when using HGAs.

Thermal noise is present in the radio Doppler measurements for a radio link having a finite SNR. During coherent tracking, thermal noise occurs at both the spacecraft transponder and at the DSN receiver. The thermal noise at the spacecraft transponder can be ignored if the SNR at the spacecraft is larger than the signal-to-noise ratio at the DSN receiver, as is typically the case due to the larger transmitter power of the DSN (~18 kW) versus the spacecraft (~20-40 W). This assumption should be checked in each application. With this assumption the thermal noise (σ_f) can be calculated as (derived from O'Dea and Kinman, 2019 or Buccino et al., 2022):

$$\sigma_f = \frac{\sqrt{2B_L}}{2\pi T_c \sqrt{P_c/N_0}} \tag{1}$$

where B_L is the bandwidth of the phase-locked loop tracking the signal, T_c is the count-time of the measurement, and P_c/N_0 is the carrier signal-to-noise spectral density ratio on a linear scale. Thus, when the SNR is low, as in the case of using LGAs or a low count-time (in some radio science applications, such as radio occultations), thermal noise becomes a dominating noise source in the error budget. Thermal noise is not a function of carrier frequency.

4 Open-Loop Data Processing

Various techniques exist to extract Doppler observables from open-loop data, which are recorded as In-phase and Quadrature samples of the downconverted antenna voltage at the DSN's OLR. These include fast-Fourier transforms (FFTs), spectral-optimized FFTs, Doppler-compensated FFTs, and software PLLs. FFTs are typically used where the signal strength or frequency is highly variable, such as in radio occultations. PLLs are more desirable for gravity observations, as they give higher precision measurements than FFTs because the bin width of the FFT does limit the measurement. However, PLLs require a more stable frequency to maintain lock. Using a PLL is analogous to measurements that come from the closed-loop receiver.

Typically, radio science observations use a spectral-optimized FFT (Paik and Asmar, 2010, Togni et al., 2021) as used in MAVEN occultations for example (Withers et al, 2018), or a PLL (Densmore, 1988) as used in Juno gravity science (Buccino et al., 2018a). This study focuses on the utilization of the PLL for precision Doppler measurements. The PLL employed is a second-order loop of Densmore (1988) integrated into the Radio Science Validation & Processing (RSVP) toolkit, successor to the STBLTY toolkit used for Galileo radio science processing (Morabito and Asmar, 1995). The PLL consists of a phase detector and loop filter, a low pass filter, and an integrator that runs over the open-loop IQ samples. The PLL is configurable to produce an output phase at a user-specified integration time and loop-bandwidth. The Doppler observable (f) at time t is then produced as a differenced-phase measurement of adjacent phase points (ϕ) over the count-time (T_c):

$$f(t) = -\frac{\phi\left(t - \frac{T_c}{2}\right) - \phi\left(t + \frac{T_c}{2}\right)}{T_c} \tag{2}$$

Three important factors must be considered when running a PLL to produce Doppler observables, particularly at low SNR: maintain a loop-SNR above the tracking threshold, minimize static phase error (SPE) in the loop, and optimize the thermal noise by producing unique phase points. The DSN closed-loop receiver can utilize a second-order loop or third-order loop. In typical DSN operations a third-order loop is utilized. The second-order loop is analogous in behavior to the second-order PLL utilized by this study - the same used in previous radio science investigations, e.g. Juno, Galileo - and thus those constraints may be applied here.

Firstly, the loop-SNR must be above the tracking threshold to acquire and maintain lock on the carrier signal in the recording. The PLL's loop-SNR (ρ_L) tracking threshold is approximately 7-10 dB. The loop-SNR is defined as the downlink carrier SNR divided by the loop bandwidth (O'Dea and Kinman, 2019):

$$\rho_L = \frac{P_c}{N_0} \cdot \frac{1}{B_L} \tag{3}$$

Secondly, to maintain this lock through regions where the frequency is changing rapidly or is unknown, the SPE must be kept below the lock threshold. In the application of the DSN's closed-loop tracking second-order loop (O'Dea and Kinman, 2019), the SPE must be kept below 30 degrees and is a function of the loop bandwidth, Doppler rate (α), and Doppler acceleration (β), which are typically caused by uncertainties in the predicted spacecraft's trajectory:

$$SPE(\text{rad}) = \frac{25\pi\alpha}{32\,B_L^2} + \left[\frac{25\pi\beta}{32B_L^2}t - \frac{125\pi\beta}{128B_L^3}\right] \tag{4}$$

Finally, to produce phase points and utilize all available SNR in the recording, a constraint is placed that the Doppler integration time is proportional to the loop bandwidth (Folkner and Border, 2013; Buccino et al. 2022):

$$B_L = \frac{1}{2T_c} \tag{5}$$

Each of these considerations places constraints on the configuration of the PLL. For example, to track a signal at 4 dB-Hz, the loop bandwidth must be 0.4 Hz to maintain the loop-SNR tracking threshold (Equation 3). Additionally, to maintain unique phase points and optimize thermal noise, the integration time should be one point every 1.25 seconds (Equation 5). The tolerable Doppler rate and acceleration would be limited per Equation 4 by the loop bandwidth (for 0.4 Hz loop bandwith, the limit to Doppler rate, assuming $\beta = 0\ Hz/s^2$ is $\alpha < 0.05\ Hz/s$) Residual Doppler rate and Doppler acceleration can be decreased or negated by phase-steering or counter-rotation of the IQ samples from the OLR using updated models of the spacecraft trajectory (Buccino et al., 2018a). It is often desirable to have an integration rate of the PLL divisible by an integer of 60, then 60-second Doppler points can be compressed from the output of the PLL with existing software. In this case, the loop bandwidth is set to 0.25 Hz and the integration time is 2 seconds, allowing for a signal at 4 dB-Hz to have a loop SNR above 10 dB and a divisible-by-60 integration time. The maximum tolerable residual Doppler rate and acceleration would be reduced (a 0.25 Hz loop bandwith would limit the Doppler rate $\alpha < 0.013\ Hz/s$, assuming $\beta = 0\ Hz/s^2$).

5 Ground System Demonstration

A test was conducted with the DSN to demonstrate the capability to make Doppler measurements at very low SNR. The DSN's DSS-25 station in Goldstone, California was placed in the same configuration as is done during a normal tracking pass where coherent Doppler measurements are taken, where instead of a spacecraft, a device called the "test translator" was placed at the final stage to provide the phase coherent downlink from the generated uplink signal. This configuration is shown in Figure 1. The X-band uplink exciter generated a 7170 MHz signal, derived from the DSN's hydrogen maser-based Frequency and Timing Subsystem (FTS). The X-band transmitter amplifies this signal through a diplexer. Typically, this signal would then be transmitted *out the horn* to the desired spacecraft. Instead, the test translator phase-coherently receives the uplink signal and multiplies it by a turnaround ratio of 880/749, typical of most deep-space X-band transponders. The test translator is equipped with a precise variable attenuator, which reduces the signal power to a level typical of reception. Now at a frequency of approximately 8424 MHz, this signal is sent back through the diplexer and into the cryogenically-cooled Low-Noise Amplifier (LNA). The signal is downconverted from a radio frequency (RF) level to an intermediate frequency (IF) level of approximately 300 MHz. The signal is then digitized through the DSN common platform: IF gain control, IF digitization, and finally flows into the digital IF switch where the Open-Loop Receiver (OLR) records the signal with In-Phase and Quadrature complex samples (Bedrossian & Rogstad, 2021).

During this test, the variable attenuator of the test translator artificially reduced the signal power such that the received SNR at the open-loop receiver was between 2 dB-Hz and 12 dB-Hz, in steps of 2 dB-Hz. Approximately 15 minutes of data were collected at 2 dB-Hz, 6 dB-Hz, 8 dB-Hz, 10 dB-Hz and 12 dB-Hz, and 30 minutes were collected at 4 dB-Hz. The OLR was configured to sample the signal at a rate of 1 kHz with 16-bit samples.

SNR measurements were made with an FFT estimation with 30 seconds of integration time. The signal was able to be tracked at each targeted SNR to within ± 0.2 dB-Hz, though the lowest targeted SNR of 2 dB-Hz was, in actuality, measured at 2.6 dB-Hz. Variations from the target are caused by fluctuations in transmitter power output. The 2.6 dB-Hz minimum led to the selection of a PLL loop-bandwidth (B_L) of 0.25 Hz. To optimize the thermal noise in the Doppler measurement, the integration time (T_c) was set to 2 seconds ($T_c = 1/2B_L$). The resulting SNR measurements and Doppler residuals (observed minus predicted) are shown in Figure 2. The root-mean-square (RMS) of the Doppler residuals was 34 mHz at 4 dB-Hz and 42 mHz at 2.6 dB-Hz. With standard frequency compression of the Doppler residuals to 60-second integration time, the resulting RMS was 1.4 mHz at 4 dB-Hz (in units of range-rate, using the conversion factor $c/2f_c$ where c is the speed of light and f_c is the carrier frequency, is 0.025 mm/s). For phase-noise dominated measurements, using phase compression over standard frequency compression will result in higher precision measurements (Buccino et al., 2022).

As expected per thermal noise theory (Section 2), as the SNR is reduced the noise in the Doppler measurement increases. Since the test was conducted on the ground, no propagation noise or antenna mechanical noise is introduced. Thus, the only remaining noise sources are thermal noise, DSN instrumental noise, and DSN FTS noise. DSN instrumental and FTS noise is negligibly small compared to thermal noise in this case. Therefore, the measured noise can be directly compared with the model for thermal noise in Eq. (1) and is shown in Figure 3. The measured performance using the digital PLL is comparable to the thermal noise model, and differences can be explained by the uncertainty in the SNR power measurements (Figure 2).

The Allan deviation (Allan, 1966) is a measure of fractional frequency stability, commonly used in clock and radio tracking performance. Using the 30 minutes of data collected at 4 dB-Hz in the ground system demonstration, the Allan deviation was computed from the residual frequencies and is plotted as a function of integration time τ in Figure 4 ($\sim 1\times10^{-12}$ at 10-sec integration time). The Allan deviation (σ_y) is proportional to white phase noise characterized by a slope of τ^{-1} as expected since this test was conducted in the absence of spacecraft instrumental noise and propagation noise.

6 Demonstration with Spacecraft

Although there have been various uses of low-SNR signals (Section 2), to the best of our knowledge none have yet reached the low single digits (~4 dB-Hz). The ground testing (Section 4) demonstrated the feasibility of such tracking. In order to test with the full link, 34-meter DSN antennas were scheduled concurrently to a primary spacecraft track on a different antenna (a configuration called a “shadow track”). The antenna is pointed off of boresight to reduce the SNR artificially. By taking advantage of the beam pattern of the antenna, the SNR can be reduced to a targeted quantity for short periods. Over longer durations, mechanical loading on the antenna changes the antenna pointing, causing the targeted SNR to vary. Nonetheless, this technique can be applied to prove the feasibility of low-SNR tracking with the full link configuration, including propagation noise, without changing the spacecraft’s command sequences. Two such tests were conducted.

The first utilized Juno spacecraft (Asmar et al., 2017) tracking in a coherent three-way mode (DSS-25 was the primary transmit antenna and DSS-35 was the secondary antenna used for the test). To reduce the SNR from the nominal level of ~40 dB-Hz to ~4 dB-Hz, a pointing offset of 71-72 millidegrees was used, placing it near the null between the primary beam and the

first side lobe. Two data segments were analyzed: the first with an SNR of 3 dB-Hz and the second with an SNR of 4.8 dB-Hz (averaged over the duration of the data span). The segments were 1 millidegree apart in pointing. Processing the open-loop data using the same configuration of the PLL from Section 4 (B_L = 0.25 Hz; T_c = 2 sec) could be performed, though the second data segment at ~3 dB-Hz had a phase cycle slips where the PLL briefly lost lock (causing a loss of ~28 seconds of data out of the 12 minute data span; the Doppler measurements affected by the cycle slips are not used in the statistical calculations that follow). These cycle slips, although unimportant for the statistics reported in this work, may be significant if they occurred during a radio science experiment and may have a loss of information depending on the timing where they occurred.The measured Doppler residual RMS at 2-second integration time (Figure 5) was 88 mHz for the first segment at 3 dB-Hz and 50 mHz for the second segment at 4.8 dB-Hz. This differs from the ground-only demonstration due to additional propagation noise sources (e.g. Earth troposphere, Earth ionosphere, and solar plasma). After data compression (frequency averaging) to 60-second integration time, the resulting RMS was 2.5 mHz at 3 dB-Hz and 1.2 mHz at 4.8 dB-Hz (the equivalent range-rate RMS is 0.045 mm/s and 0.021 mm/s, respectively).

The second utilized the New Horizons spacecraft (Tyler et al., 2009) tracking in a non-coherent one-way mode with DSS-25 receiving (the New Horizons Ultra Stable Oscillator provided the frequency reference). Utilizing an antenna pointing offset of 60 millidegrees resulted in an SNR of 4.5 dB-Hz. Again, with the same PLL configuration (B_L = 0.25 Hz; T_c = 2 sec), the Doppler residual RMS was measured to be 32 mHz at a 2-second integration time (Figure 6). The data collected were less than 5 minutes in duration, yielding less than 5 Doppler points at a 60-second integration time. Therefore 60-second integration statistics are not reported due to the low number of points. Note this is improved over the Juno result (50 mHz at 4.8 dB-Hz), however, this is nearly entirely due to the measurement geometries where Juno was affected by higher levels of plasma noise during data collection.

7 Conclusion

Doppler observable measurements are used for numerous applications. In this work, we have demonstrated that the same measurements typically taken at high SNR can also be made at low-SNR levels by utilizing the Open-Loop Receiver of the Deep Space Network at the cost of increased thermal noise in the link. Signal processing of open-loop data with a phase-locked loop was used to generate Doppler observable measurements. Ground testing demonstrated that reliable tracking was achieved at an SNR of ~4 dB-Hz. Doppler measurement noise was consistent with thermal noise theory. Flight demonstrations with the Juno spacecraft (coherent tracking) and New Horizons (noncoherent 1-way tracking with USO reference) confirmed the tracking ability using a full link configuration with a spacecraft. When signal levels were reduced below 4 dB-Hz with flight demonstration, tracking became less reliable and cycle slips occured. For the 60-second integration time, Doppler measurement noise was <0.1 mm/s in units of range-rate. For applications of this work, it is crucial to account for all potential noise sources (e.g., variable solar plasma noise, Earth troposphere, antenna mechanical), as was seen in spacecraft demonstrations where Doppler measurement precision was variable between the two tests. Furthermore, it is important to consider the effect of residual Doppler rate and acceleration, primarily function of how well the spacecraft trajectory is predicted to be known, in applications of low-SNR signal tracking. Lower tracking bandwidths needed to maintain lock also require lower residual Doppler rate and acceleration. Although lower Doppler rate and accelerations may be required to precisely track, the science information contained within the data may still contain

317 useful information for the analysis of gravitiational fields, ionosphere and atmosphere via radio
318 occultations, and further improving the spacecraft's trajectory.

319 **Acknowledgments**

320 The authors would like to thank Dong Shin and Steve Olson of the Deep Space Network for
321 coordinating and executing the ground-system demonstration. The authors would like to thank
322 the Europa Clipper project and the Juno project at the Jet Propulsion Laboratory as well as the
323 New Horizons project at the Johns Hopkins University Applied Physics Laboratory for their
324 support of this effort. PW acknowledges support from NASA via the MAVEN, Juno, and Europa
325 Clipper projects.
326
327 This work was carried out at the Jet Propulsion Laboratory, California Institute of Technology,
328 under a contract with the National Aeronautics and Space Administration (80NM0018D0004).
329 Government sponsorship acknowledged. PT and MZ are grateful to the Italian Space Agency
330 (ASI) for financial support through Agreement No. 2021-13-HH.O in the context of NASA's
331 Europa Clipper mission.
332

334 **Data Availability Statement**

335 The open-loop test data and processed Doppler observable measurements are provided in a
336 corresponding dataset with this publication on Zenodo (Buccino, 2023).

337 **References**

338 Allan, D.W. Statistics of atomic frequency standards. *Proc. IEEE* 1966, 54, 221–230.

339 Asmar, S. W., Armstrong, J. W., Iess, L., & Tortora, P. (2005). Spacecraft Doppler tracking:
340 Noise budget and accuracy achievable in precision radio science observations. *Radio*
341 *Science*, *40*(2), 1-9.

342 Asmar, S. W., Lazio, J., Atkinson, D. H., Bell, D. J., Border, J. S., Grudinin, I. S., ... & Preston,
343 R. A. (2019). Future of planetary atmospheric, surface, and interior science using radio and laser
344 links. *Radio Science*, *54*(4), 365-377.

345 Asmar, S. W., Bolton, S. J., Buccino, D. R., Cornish, T. P., Folkner, W. M., Formaro, R., ... &
346 Simone, L. (2017). The Juno gravity science instrument. *Space Science Reviews*, *213*(1), 205-
347 218.

348 Barbaglio, F., Armstrong, J. W., & Iess, L. (2012, October). Precise Doppler Measurements for
349 Navigation and Planetary Geodesy Using Low Gain Antennas: Test Results from Cassini.
350 In *23rd International Symposium on Space Flight Dynamics, Pasadena, CA*.

351 Barbinis, E. (2016). Titan Gravity Science Experiment Raw Data Archive, CO-SSA-RSS-1-
352 TIGR19-V1.0, NASA Planetary Data System. https://pds-
353 atmospheres.nmsu.edu/data_and_services/atmospheres_data/Cassini/inst-rss.html

354 Bedrossian, A., & Rogstad, S. (2021). Open-Loop Radio Science. In *DSN Telecommunications*
355 *Link Design Handbook* (Vol. 202, pp. 810-005). Rev. E. Jet Propulsion Laboratory.

Border and Folkner, "Thermal Noise Contribution to Doppler Measurement Error", JPL Interoffice Memorandum JSB-3-09-18, 18 Sept 2013.

Buccino, D. R., Kahan, D. S., Yang, O., & Oudrhiri, K. (2018, January). Extraction of Doppler observables from open-loop recordings for the Juno radio science investigation. In *2018 United States National Committee of URSI National Radio Science Meeting (USNC-URSI NRSM)* (pp. 1-2). IEEE.

Buccino, D., Kahan, D., Yang, O., & Oudrhiri, K. (2018, March). Initial operations experience and results from the Juno gravity experiment. In *2018 IEEE Aerospace Conference* (pp. 1-8). IEEE.

Buccino, D., Border, J. S., Folkner, W. M., Kahan, D., & Le Maistre, S. (2022). Low-SNR Doppler Data Processing for the InSight Radio Science Experiment. *Remote Sensing*, *14*(8), 1924.

Buccino, D., (2023) "Corresponding Dataset for Precision of Spacecraft Doppler Tracking at Low Signal-to-Noise Ratios" [Data set]. https://doi.org/10.5281/zenodo.7703138

Dehant, V., Le Maistre, S., Baland, R. M., Bergeot, N., Karatekin, Ö., Péters, M. J., ... & Folkner, W. M. (2020). The radioscience LaRa instrument onboard ExoMars 2020 to investigate the rotation and interior of mars. *Planetary and Space Science*, *180*, 104776.

Densmore, A.C., A Digitally Implemented Phase-Locked Loop Detection Scheme for Analysis of the Phase and Power Stability of a Calibration Tone. *TDA Progress Report* 42-93, 1988.

Durante, D., Hemingway, D. J., Racioppa, P., Iess, L., & Stevenson, D. J. (2019). Titan's gravity field and interior structure after Cassini. *Icarus*, *326*, 123-132.

Felici, M., Withers, P., Smith, M. D., González-Galindo, F., Oudrhiri, K., & Kahan, D. (2020). MAVEN ROSE observations of the response of the Martian ionosphere to dust storms. *Journal of Geophysical Research: Space Physics*, 125, e2019JA027083.

Hinson, D. P., Flasar, F. M., Kliore, A. J., Schinder, P. J., Twicken, J. D., & Herrera, R. G. (1997). Jupiter's ionosphere: Results from the first Galileo radio occultation experiment. *Geophysical Research Letters*, *24*(17), 2107-2110.

Iess, L., Di Benedetto, M., James, N., Mercolino, M., Simone, L., & Tortora, P. (2014). Astra: Interdisciplinary study on enhancement of the end-to-end accuracy for spacecraft tracking techniques. *Acta Astronautica*, *94*(2), 699-707.

Konopliv, Alex S., et al. (2011), "The Dawn gravity investigation at Vesta and Ceres," *Space Science Reviews*, 163.1-4 , 461-486.

Lainey, V., Casajus, L. G., Fuller, J., Zannoni, M., Tortora, P., Cooper, N., ... & Zhang, Q. (2020). Resonance locking in giant planets indicated by the rapid orbital expansion of Titan. *Nature Astronomy*, *4*(11), 1053-1058.

Mazarico, E.; Buccino, D.R.; Castillo-Rogez, J.; Dombard, A.; Genova, A.; Hussmann, H.; Kiefer, W.S.; Lunine, J.I.; McKinnon, W.B.; Nimmo, F.; et al. The Europa Clipper Gravity/Radio Science Investigation. In *Proceedings of the Lunar and Planetary Science Conference*, Online, 15–19 March 2021; p. 1784.

Morabito, D.D. and Asmar, S.W., Radio Science Performance Analysis Software. *TDA Progress Report* 42-120, 1995.

Moyer, T.D. Formulation for Observed and Computed Values of Deep Space Network Data Types for Navigation; *John Wiley & Sons*: New York, NY, USA, 2005; Volume 3.

O'Dea, A., & Kinman, P. (2019). Doppler Tracking. In *DSN Telecommunications Link Design Handbook* (Vol. 202, pp. 810-005). Rev. C. Jet Propulsion Laboratory.

Paik, Meegyeong, and Sami W. Asmar (2010), "Detecting high dynamics signals from open-loop radio science investigations," *Proceedings of the IEEE* 99.5, 881-888.

Tyler, G. L., Linscott, I. R., Bird, M. K., Hinson, D. P., Strobel, D. F., Pńtzold, M., ... & Sivaramakrishnan, K. (2009). The New Horizons radio science experiment (REX). In *New Horizons* (pp. 217-259). Springer, New York, NY.

Togni, A., Zannoni, M., Casajús, L. G., & Tortora, P. (2021, June). An FFT-based method for Doppler observables estimation in Deep Space tracking. In *2021 IEEE 8th International Workshop on Metrology for AeroSpace (MetroAeroSpace)* (pp. 294-299). IEEE.

Withers P. et al. (2018), "First ionospheric results from the MAVEN Radio Occultation Science Experiment (ROSE)," *Journal of Geophysical Research*, 123, 4171-4180

Withers, P., Felici, M., Mendillo, M., Moore, L., Narvaez, C., Vogt, M. F., ... & Jakosky, B. M. (2020). The MAVEN radio occultation science experiment (ROSE). *Space Science Reviews*, *216*(4), 1-49.

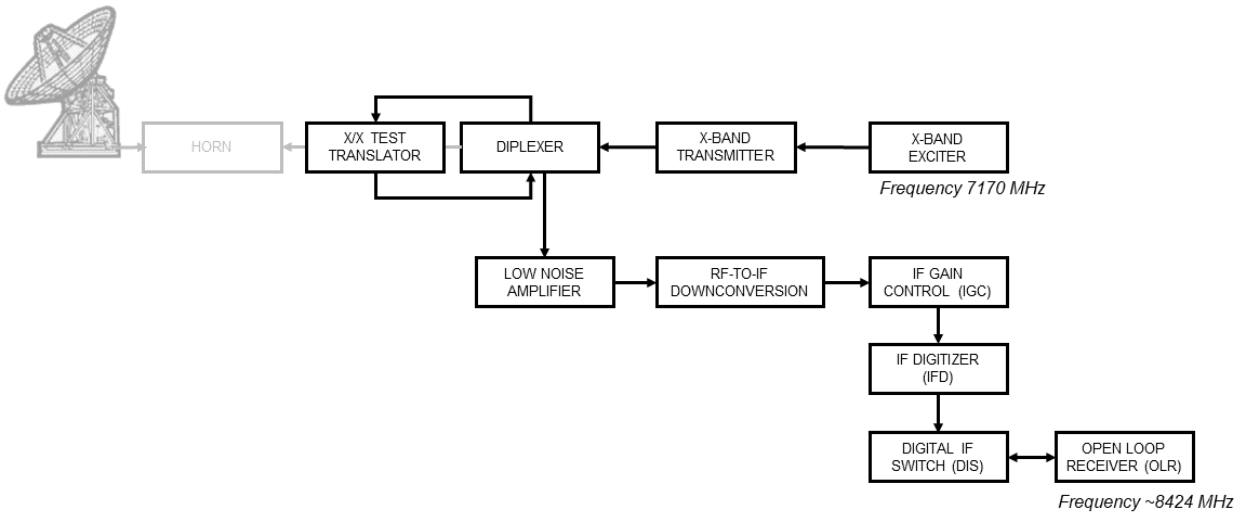

Figure 1. Configuration of the DSS-25 antenna in Goldstone, California to demonstrate Doppler tracking capabilities at very-low SNR. In lieu of a spacecraft, the test translator device with a precise variable attenuator was utilized to convert the uplink frequency to a downlink frequency and adjust the signal power level to the desired levels of 2 dB-Hz to 12 dB-Hz.

421

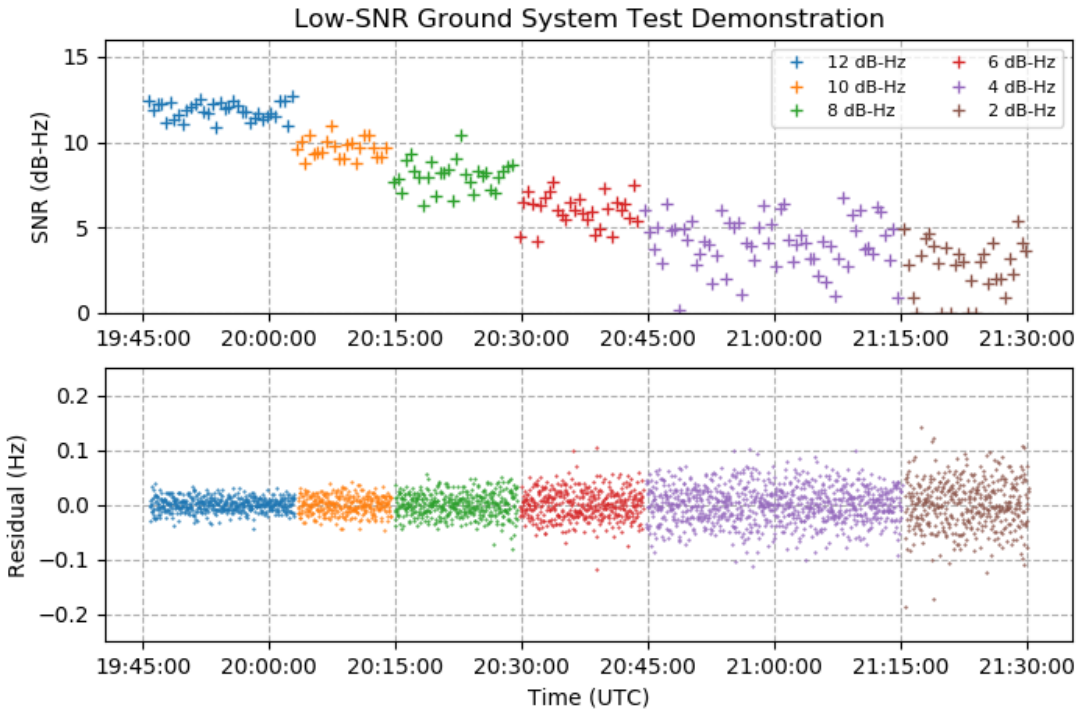

422

423 **Figure 2**. Measured SNR (top) and measured Doppler residuals (bottom) during the ground
424 demonstration of low-SNR tracking capabilities. SNR was measured using an FFT at 30 second
425 integration time and Doppler residuals were estimated using a PLL at 2-second integration time.
426

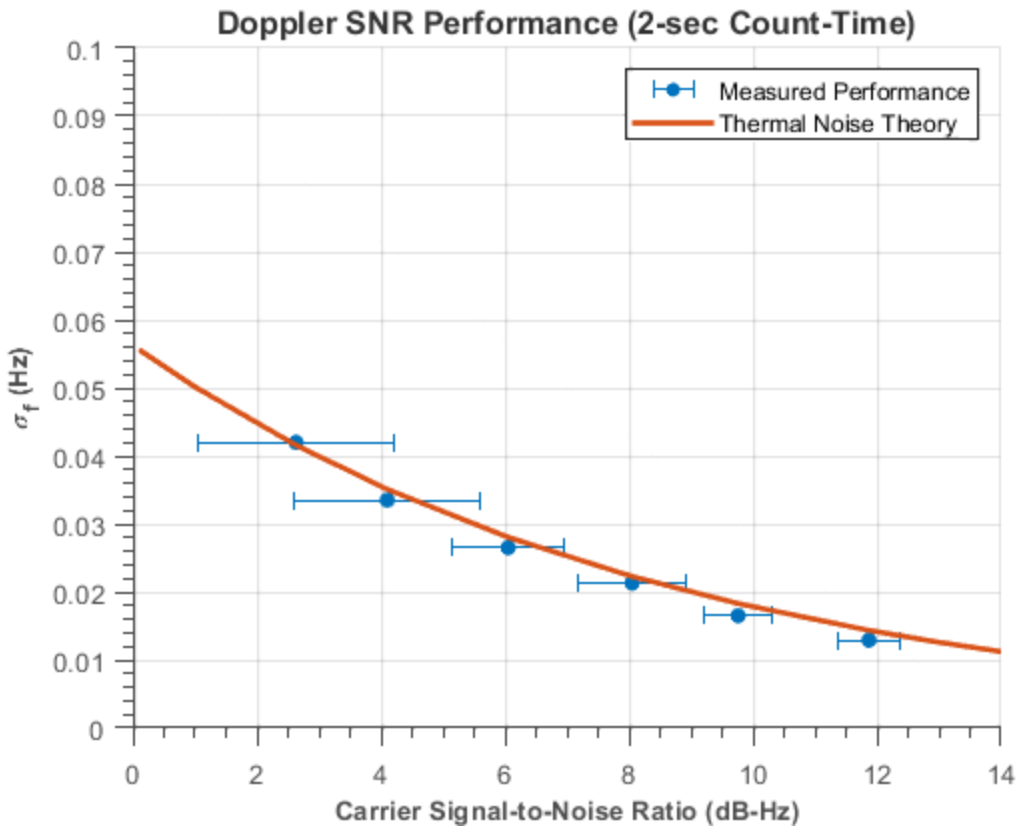

Figure 3. Standard deviation of Doppler residuals as function of SNR during the ground system demonstration of low-SNR tracking capabilities, estimated using a PLL (B_L = 0.25 Hz, T_c = 2 sec). The error bars are the 1-sigma standard deviation of the power measurement from Figure 2. The measurements are compared with a model of thermal noise from Eq. (1). The measurements are taken in the absence of propagation noise and spacecraft instrumental noise.

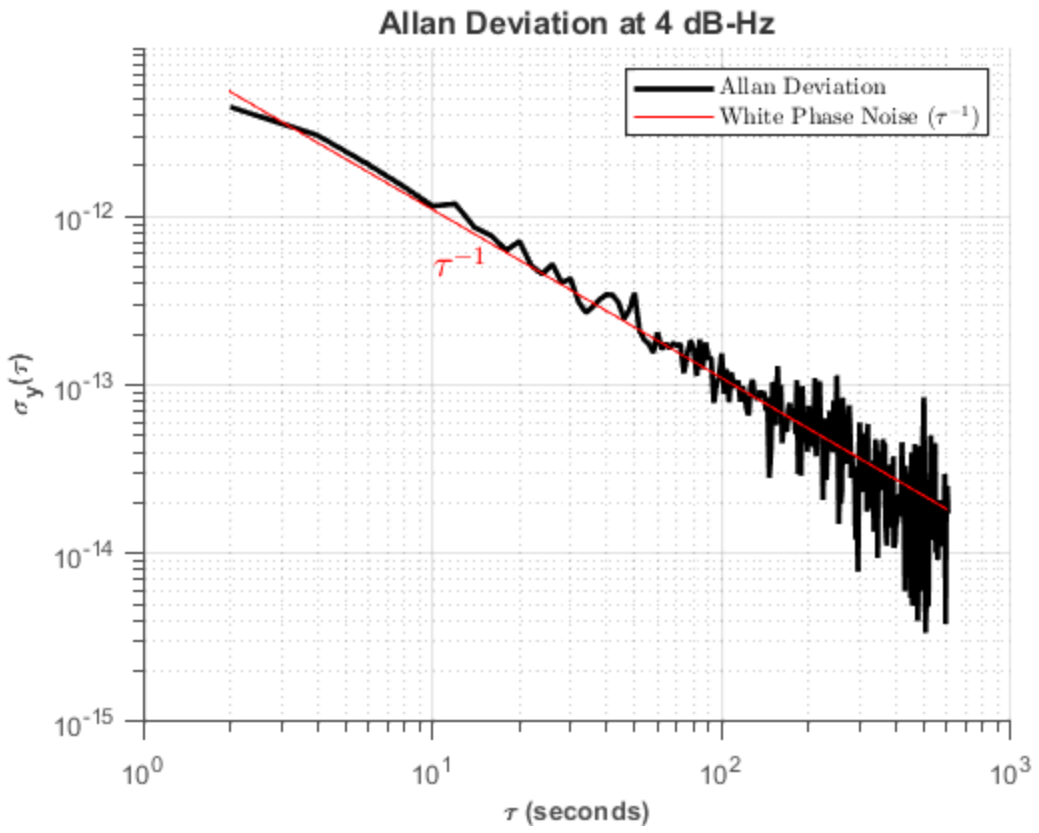

Figure 4. Allan deviation of the Doppler residuals at an SNR level of 4 dB-Hz from the ground system demonstration of low-SNR tracking capacities. The measured Allan deviation is proportional to τ^{-1}, indicating the signal is characterized by white phase noise.

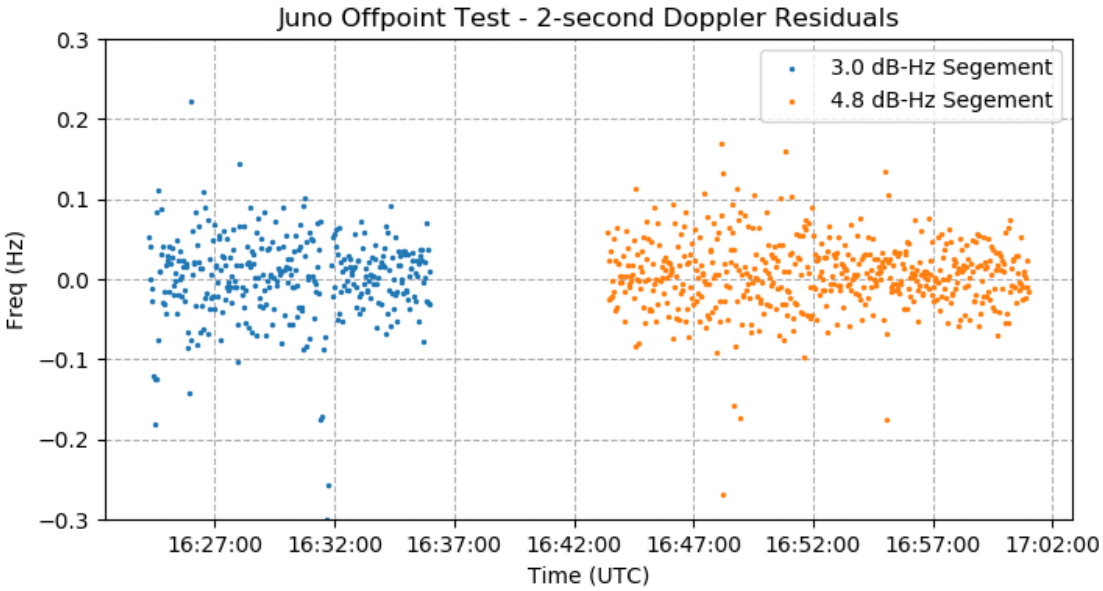

Figure 5. Coherent three-way Doppler residuals from Juno at 2-second integration time while artificially reducing the received SNR by introducing a pointing offset into the DSN antenna. The first segment was collected with an average SNR of 3 dB-Hz (blue) and second segment was collected with an average SNR of 4.8 dB-Hz (orange).

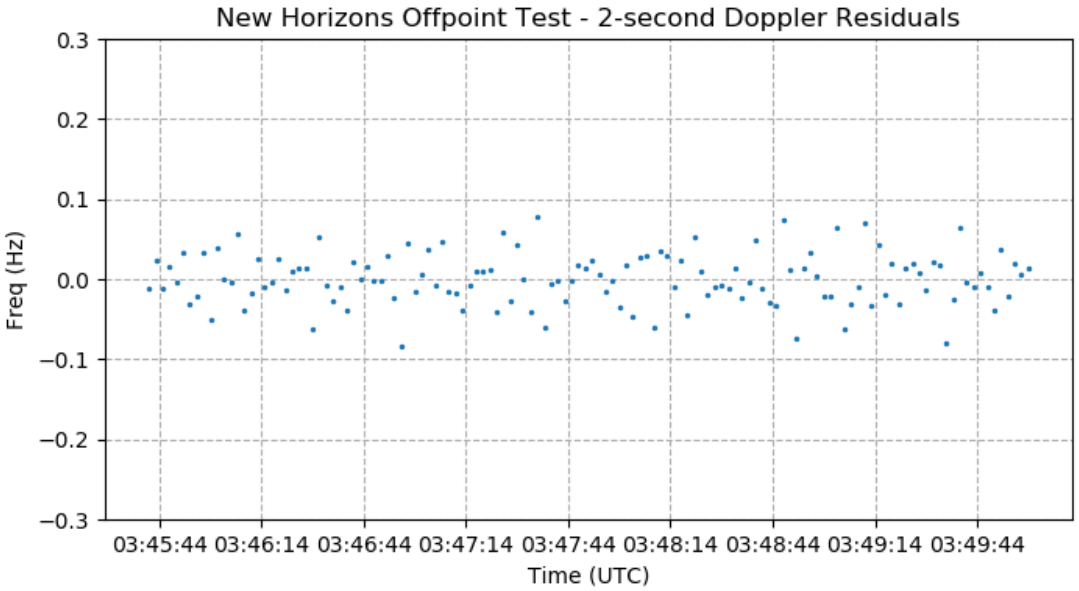

Figure 6. Non-coherent one-way Doppler residuals from New Horizons at 2-second integration time while artificially reducing the received SNR by introducing a pointing offset into the DSN antenna. The average SNR during this segment of data was 4.5 dB-Hz.